AIP | Review of Scientific Instruments

A novel system of coils for magnetobiology research

L. Makinistian

Citation: Review of Scientific Instruments **87**, 114304 (2016); doi: 10.1063/1.4968200
View online: http://dx.doi.org/10.1063/1.4968200
View Table of Contents: http://scitation.aip.org/content/aip/journal/rsi/87/11?ver=pdfcov
Published by the AIP Publishing

A novel system of coils for magnetobiology research

L. Makinistian[a)]
Department of Physics and Instituto de Física Aplicada (INFAP), Universidad Nacional de San Luis, Consejo Nacional de Investigaciones Científicas y Técnicas, Ejército de los Andes 950, 5700 San Luis, Argentina

(Received 29 July 2016; accepted 8 November 2016; published online 29 November 2016)

A novel system of coils for testing *in vitro* magnetobiological effects was designed, simulated, and built. Opposite to what is usual, the system generates a controlled gradient of magnetic field. This feature is introduced to allow the assessment of multiple values of the field in a single experiment. The apparatus consists of two flattened orthogonal coils, which permit independent control of two of the spatial components of the field. Geometry of design, combined with the use of a standard multi-well microplate for cellular culture, allows for simultaneous testing of 96 different field conditions. The system, intended to increase the efficiency of evaluating biological effects throughout ranges of the field parameters, was fully characterized injecting DC currents to the coils (i.e., generating static magnetic fields) in order to assess the spatial distribution of both the field's and field-gradient's components. Temperature load was carefully evaluated and the maximum values of 350 μT and 9 μT/mm (for the field and its gradient) could be generated without excessive heating of the cellular cultures. *Published by AIP Publishing.* [http://dx.doi.org/10.1063/1.4968200]

I. INTRODUCTION

During the last few decades, there has been an ever increasing interest in the biological effects of static and extremely low frequency magnetic fields (SMF and ELF-MF).[1–4] In regards to *in vitro* experiments, it is to be noted that the vast majority of ELF-MF studies used field-generating systems that guaranteed a highly uniform MF. While Helmholtz coils (HC) have been the classic, most utilized resource,[5–7] other configurations with even better performance have also been developed.[8,9] As to SMF, there have also been studies using homogeneous fields generated by HC[10,11] or superconducting magnets,[12,13] but the use of inhomogeneous fields from permanent magnets has been more frequent[14–16] (presumably because of their low cost).

Even though the use of a homogeneous field has clear advantages (i.e., measurement is less difficult and spatial gradients of the field are null, so there is one less variable to control/assess), we note here that it also has a disadvantage, namely, that a single value of the field is evaluated per experiment. Thus, if the aim of the study is to explore the effect throughout an entire range of, say, the field's intensity, several experiments must be performed: one for each of the values to be tested. While this approach does yield valuable results, it runs with a risk: missing the observation of significant changes that could have been observed had a little variation of the exposure parameters been tested. Indeed, a thorough review of the literature[1] shows that there are both abundant experimental evidence and robust theoretical arguments that demonstrate that "slight" changes of the field parameters can prevent a biological effect from being elicited or even induce the opposite one. For instance, in experiments with E. coli bacteria exposed to SMF, Binhi *et al.*[17] showed that increments of as low as 10 μT changed from effect to no-effect and back to effect but of the opposite sign. This non-linearity and non-monotonicity (i.e., the existence of amplitude windows)[18,19] make it desirable to conduct experiments that would screen throughout a range of the field intensity rather than evaluating a sharply defined, single value. Permanent magnets could be a solution, since they provide with a range of fields distributed in space; however, there is no control of the field intensity or of the way fields fade away from the magnet. Hence, it would be convenient to use a field-generating system that would generate a controlled gradient of magnetic field.

As a step in this direction, we designed, simulated, built, and fully characterized with DC currents (i.e., generating SMF), a system of coils that, upon combination with a standard 96 well microplate for cellular culture (Costar 3599, CORNING, Corning, NY), allows for testing multiple field exposures in a single experiment.

II. SYSTEM DESIGN AND SIMULATION

A. Mechanical and electrical details

The device presented here consists of two flattened orthogonal coils according to the schematics of Figures 1(a)–1(c), while Figure 1(d) is a photo of the realization of the system.

Both coils have an air core and are wound around custom-made polyvinyl chloride (PVC) supports that are themselves rigidly mounted onto an acrylic base 8 mm thick. The base has holes of 6 mm diameter every 20 mm all throughout its surface, in a square grid (see Fig. 1(d)), which allow better air flow inside an incubator. All screws and bolts are of bronze, i.e., non-ferromagnetic, in order to prevent their magnetization with time and the concurrent distortion of the generated fields. An acrylic shelf is mounted so cells in a standard 96 well microplate are effectively positioned within a millimeter of the plane of symmetry of the system. An acrylic frame is fixed onto the shelf so that the microplate is located precisely (within less

a)Author to whom correspondence should be addressed. Electronic mail: lmakinistian@unsl.edu.ar. Tel.: +54-266-4520329 (ext. 3080). Fax: +54-266-4447462.

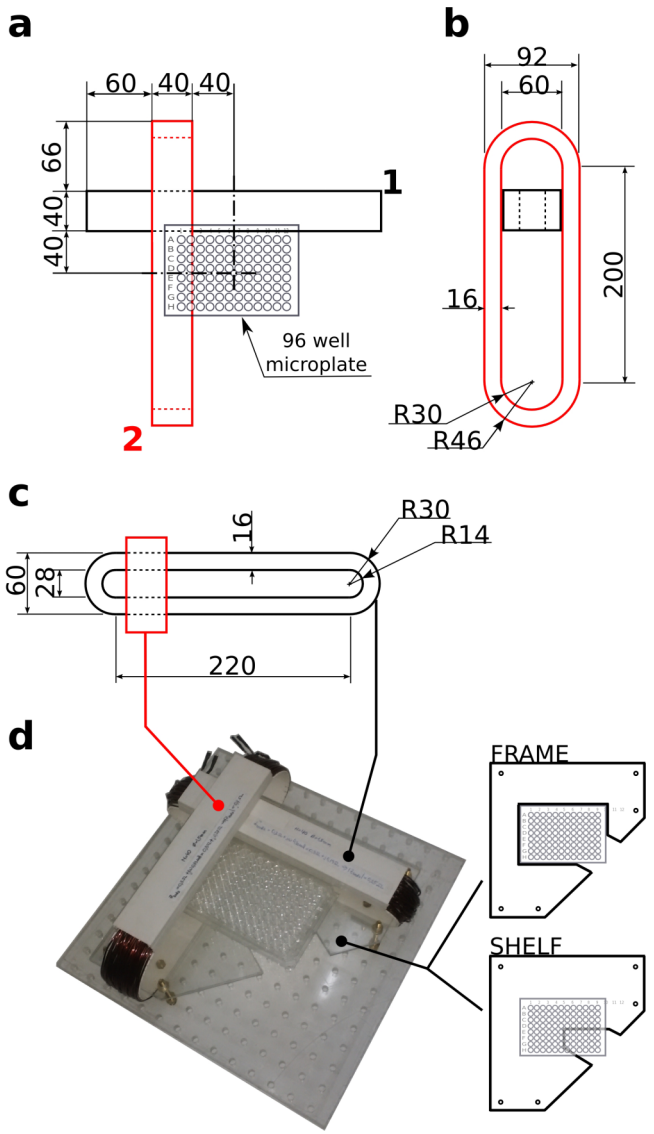

FIG. 1. (a)–(c): Dimensions and relative position of the two coils (all in mm). (d): A photo of the system, where the multi-well microplate, the acrylic base, shelf for the microplate, the positioning frame (exactly on top of the shelf), and the bronze screws and bolts can be seen.

than a millimeter error) at the same position with respect to the coils in different experiments: this positioning frame is of paramount importance since fields are highly inhomogeneous (both the ones generated by the coils and the ones intrinsic to incubators[20]). A few millimeters displacement from an experiment to another, attempting a replication, may yield different results.

Both coils were built with N = 40 windings of a copper wire 1.450 mm in diameter (AWG 15). Resistance and inductance of the coils were measured with an LCR-916 impedance meter (GW Instek, New Taipei City, Taiwan) using a testing frequency of 100 Hz: $R_1 = R_2 = 0.3\ \Omega$, $L_1 = 0.43$ mH, and $L_2 = 0.30$ mH.

Although the system presented here somewhat resembles that of a US patent,[21] both systems show important differences. (1) The system by Kaufman *et al.* consists of two orthogonal coils with a rectangular shape (not oblong), with similar height and width, in the order of 1 m; also, unlike the flattened coils in this work, they are centered: each lies on one of the planes of symmetry of the other. (2) Their coils are designed for the transmission of homogeneous radiofrequency fields, not a controlled gradient of the magnetic field (MF). (3) Their invention is intended for magnetic resonance imaging, not *in vitro* experiments. Therefore, to the best of this author's knowledge, no system similar to the one presented here has been reported before.

B. Computational details

The MF at each of the locations in which a field measurement was done (see below) was computed by the Biot-Savart law (implemented in a custom code written in Python). Figure 2(a) shows the three-dimensional model of the two coils used to simulate the field generated by the device, in which dimensions are exactly those of the schematics in Figure 1. Each coil was represented by N = 40 oblong loops (corresponding to the 40 windings of the cooper wire that make up each coil), each of which was formed by two straight and parallel lines connected to each other by two half-circular arches with opposite, facing concavities. In term, each of these 40 loops was discretized into 160 nodes, where each node had a vector nature and represented a discrete version of a current differential. This degree of discretization (160 nodes per loop) yielded a convergence better than 0.1 μT for the integrated fields.

Naturally, the fine details of the result of the simulation depend on the exact location of the loops of current in space.

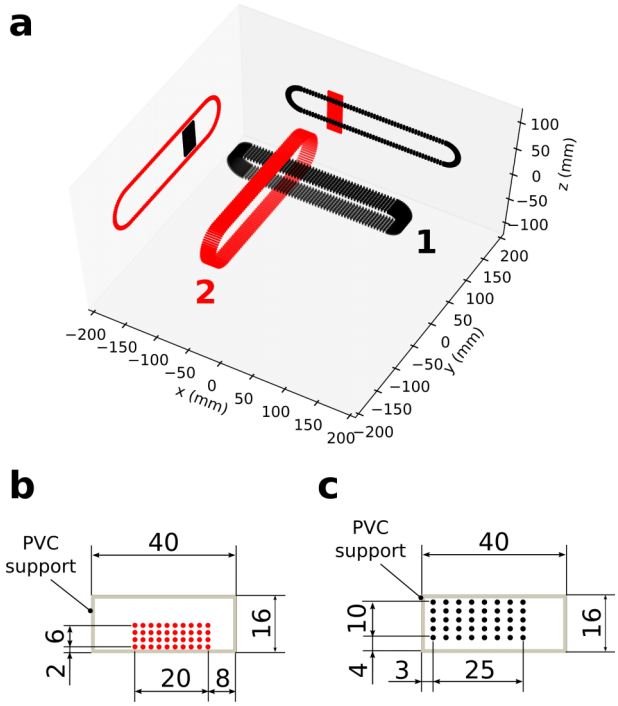

FIG. 2. (a): Three-dimensional model of the two coils; each coil is represented by N = 40 oblong loops, each of which is discretized into 160 nodes. Each node has a vector nature and represents a "current differential." Ultimately, the magnetic field is computed by the Biot-Savart law by integrating (adding) the contributions of all of the nodes, from all of the loops. (b) and (c): Exact position of the 40 loops of current for coils 2 and 1, respectively, with respect to their PVC supports.

Here, the exact positions of the loops within the PVC supports, which entered the model exclusively by defining the region of space inside which the loops of currents had to be, were adjusted (by trial and error) to better approximate the experimental measurements. These locations are specified in Figures 2(b) and 2(c) (coils 2 and 1, respectively). It is clear that the current loops were not centered inside their respective PVC supports. This is justified on the basis that a close inspection of the actual device shows that the windings of the copper wire were, indeed, not perfectly centered. Moreover, it should be noted that the actual coils are not perfect, parallel loops, but imperfect single (continuous) spirals in space. Thus, a perfect match between simulation and measurements should not be expected. In spite of this, we show below that an acceptable agreement was reached.

III. SYSTEM PERFORMANCE

A. B-field measurement

Due to the field's gradient, it is clear that a single measurement of it at some point of space would be insufficient. Instead, a two-dimensional map of the field must be assessed exactly at the height at which the cells will be resting during the experiments. To this end, the field intensity in the 3 directions of space (x, y, z) was measured with an HCM5883L 3-axis magnetometer (Honeywell, New Jersey, NY) connected to a personal computer (PC) through an Arduino Leonardo board.[22] The magnetometer package dimensions are $3.0 \times 3.0 \times 0.9$ mm (so the sensors themselves are even smaller, which makes them appropriate for the 4×4 mm grid that was chosen for assessing the field maps in this work) and has a field resolution of 0.2 μT. The magnetometer was calibrated using a 300 mm diameter Helmholtz coil (Model TG-13, UCHIDA, Tokyo, Japan) with a field generating factor of 7.80×10^{-4} T/A, injected with current from a programmable DC power supply (Rigol DP1308A, Beaverton, OR) with a ripple lesser than 500 μA_{rms}. The magnetometer was manually placed on each of the points of a 4×4 mm grid (i.e., a map of 120×80 mm contains $31 \times 21 = 651$ pixels, with three readings per pixel: B_x, B_y, B_z) printed on a sheet of paper and taped to a 3 mm thick acrylic piece placed on top of the shelf. Thus, measurements were made at the level the cells would rest. The magnetometer sent the three components of the MF (B_x, B_y, B_z) sequentially to the PC, so that three maps are measured at once: one for each component of the field. For convenience, the intensity of the field $|\mathbf{B}| = (B_x^2 + B_y^2 + B_z^2)^{1/2}$ was calculated from the measured components and is also plotted in the next figures.

B. Background field

Before currents were injected to the coils the background field was measured. Care was taken not to have ferromagnetic objects or structures within approximately 1 m from the place all measurements were carried out. Figure 3 shows the average of 5 measurements of the background field. It can be seen that all values of the field intensity $|\mathbf{B}|$ are approximately between 22 μT and 24 μT. This is in excellent agreement with the value

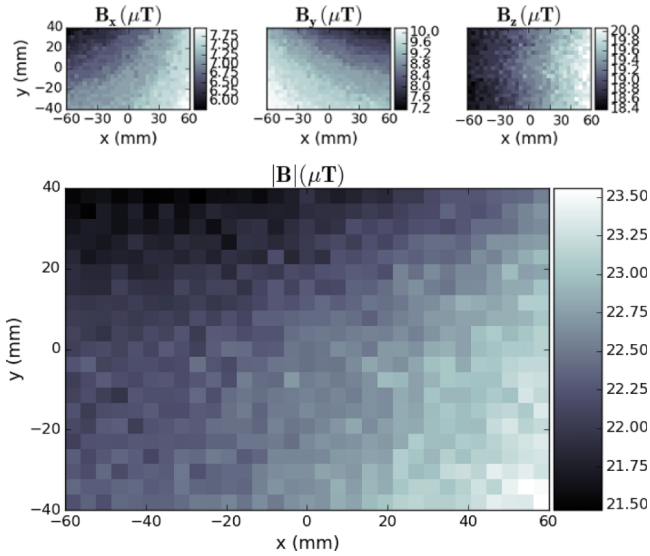

FIG. 3. The three components (B_x, B_y, B_z) and the total intensity ($|\mathbf{B}|$) of the background field (average of five measurements), mostly due to the Earth's magnetic field.

of 23.2629 μT for the Earth MF that the National Centers for Environmental Information[23] estimate when the coordinates of the city of San Luis, Argentina (33.27 S 66.35 W, 709 m above sea level), where the measurements took place, are plucked into their geomagnetic models (for 15 December 2015). It is noted that even though the background homogeneity was around 95%, in order not to lose accuracy unnecessarily, its subtraction from the measurements of the energized coils was performed pixel-by-pixel. It is worth mentioning here that a detailed knowledge of the background is of paramount importance, since it could be the cause of failure to reproduce experiments otherwise "identical."

While all the measurements in this work were done outside an incubator, in a concrete experiment with cellular cultures the background to be measured ought to be that inside the incubator, precisely throughout the region of the incubator at which the cell cultures will be placed. Inhomogeneities had been proven to be significant between locations just a few centimeters away.[20] This fact poses a profound question regarding the comparability of experiments in which the background fields were not adequately assessed.[24]

C. Generated B-field

Figure 4 shows the field resulting from injecting 1 A of DC current to coil 1 (Fig. 4(a)) and to coil 2 (Fig. 4(b)). It is important to notice that first, the map of the background field was measured (five times, with both coils unenergized, see Fig. 3). Next, the fields injecting 1 A were measured (also, five times), and finally, what is shown in Figure 4 is the result of subtracting the average background from the average fields measured with the coils energized. It can be seen that the field generated by a coil is almost entirely perpendicular to it, but as the distance increases, the other components turn up non-negligible. The white circles overlapping on top of the field total intensity ($|\mathbf{B}|$) indicate the (x, y)-position of the wells of a 96 well microplate.

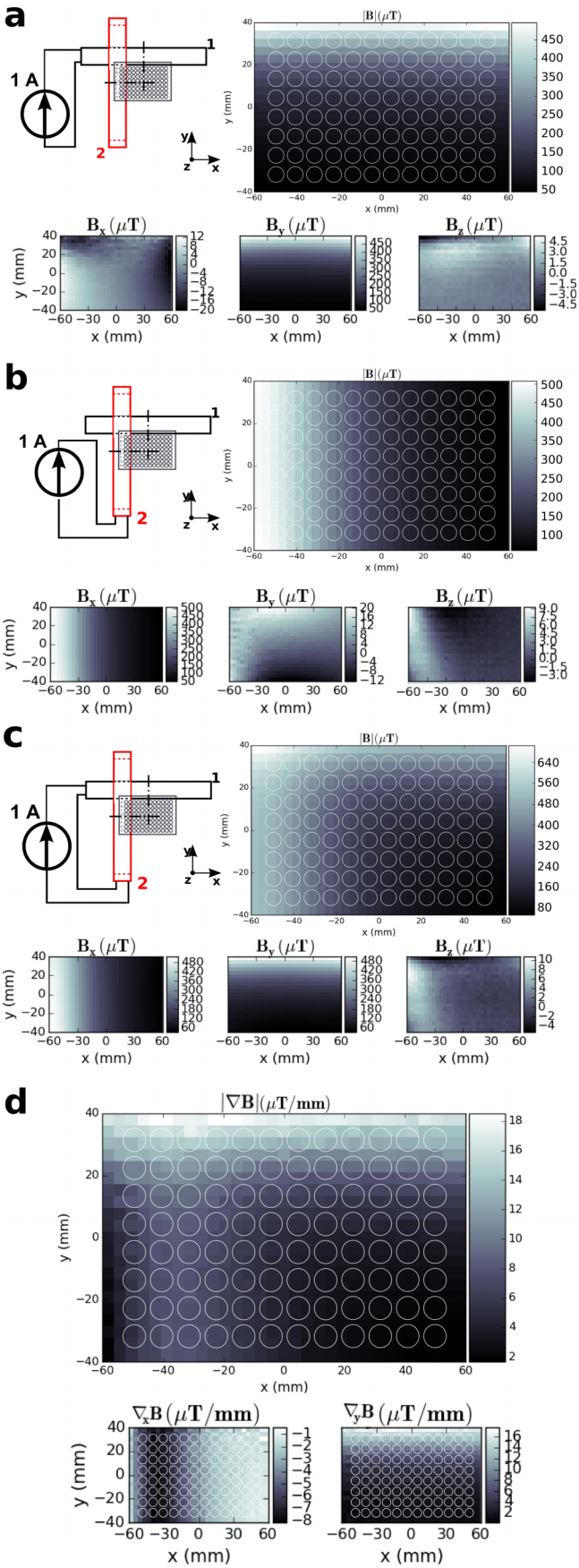

FIG. 4. Measured magnetic fields with 1 A injected to coil 1 (a), coil 2 (b), and their vector addition (c). (d): Field gradient strength, $|\nabla \mathbf{B}|$, and principal components, $\nabla_x B$ (due to coil 2) and $\nabla_y B$ (due to coil 1). Wells' positions of a 96 well microplate are indicated by the white circles.

Figure 4(c) shows the vector addition of the fields generated by the two coils. When both coils are energized (Fig. 4(c)), it is clear that the total field is not perpendicular to either of the coils. Tables S1-S3 (supplementary material) show values of the field components and total intensity for the three cases: only coil 1 energized, only coil 2 energized, and both coils energized, respectively. The most relevant field gradient components were calculated as $(B_{i,j} - B_{i-1,j})/4$ mm and $(B_{i,j} - B_{i,j-1})/4$ mm for $\nabla_x B$ (coil 2) and $\nabla_y B$ (coil 1), respectively. When both coils are energized, the total gradient intensity, $|\nabla \mathbf{B}| = [(\nabla_x B)^2 + (\nabla_y B)^2]^{1/2}$, becomes that of Figure 4(d) (Table S4, supplementary material).

In Figure 5(a), the strength of the fields of Figures 4(a) and 4(b) is re-plotted but in a three dimensional (3D) plot, while Figure 5(b) shows the net field intensity upon energizing both coils (Fig. 4(c)). Figures 5(c) and 5(d) show the main field gradient components and the gradient intensity, respectively (Fig. 4(d)). Here, it is to be noted that being a discrete derivative, the experimental computation of the gradient yields rather "noisy" surfaces; this could be enhanced by averaging a greater number of measurements and by measuring with a greater spatial resolution. Figures 5(e)–5(h) are the simulated versions of Figures 5(a)–5(d), respectively: a good qualitative agreement is evident (here, the simulations of the gradients do not show the "noise" present in the measurements, as expected). In Figures 6(a) and 6(b), cuts of the fields for x = 0 mm and y = 0 mm, respectively, illustrate how for a row or for a column of wells one of the fields is almost constant and the other changes substantially. Figures 6(c) and 6(d) show cuts of the MF gradient for x = 0 mm and y = 0 mm. In Figures 6(a)–6(d), the continuous lines correspond to the simulated fields while the symbols correspond to the actual measurements: an agreement is achieved within ~25% or less (depending on the point chosen to compare). In order to appreciate the inhomogeneity of the field also at the end-sides of the microplate, Figures 6(e) and 6(f) show the main components (B_{1y} and B_{2x}) and the total intensity ($|B|$) for x = ±60 mm and for y = ±40 mm, respectively (data for x = 0 mm and y = 0 mm are same as in Figures 6(a) and 6(b) but are plotted again for comparison purposes). While for the sake of clarity no error bars or continuous simulation curves were plotted in Figures 6(e) and 6(f), the complete sets of data can be found in Fig. S1 of the supplementary material.

D. Temperature load

Given that coils' resistances are $R_1 = R_2 = 0.3\ \Omega$ (and that the inductive part of the complex impedance does not produce heating), the total Joule effect (I^2R, where I is the current) upon injection of 1 A to both coils is 0.6 W. Besides knowing this heating power, it is critical to measure the actual increment of the temperature the cultures will be exposed to during operation of the system. This elevation is determined by a complex heat flow due to air convection inside the incubator and ultimately heat conduction from humid air to cell media (both directly through their interface and through the microplate acrylic material). Furthermore, it should be expected that the temperature load will be different for different wells: the closest ones to the coils being the ones facing the highest

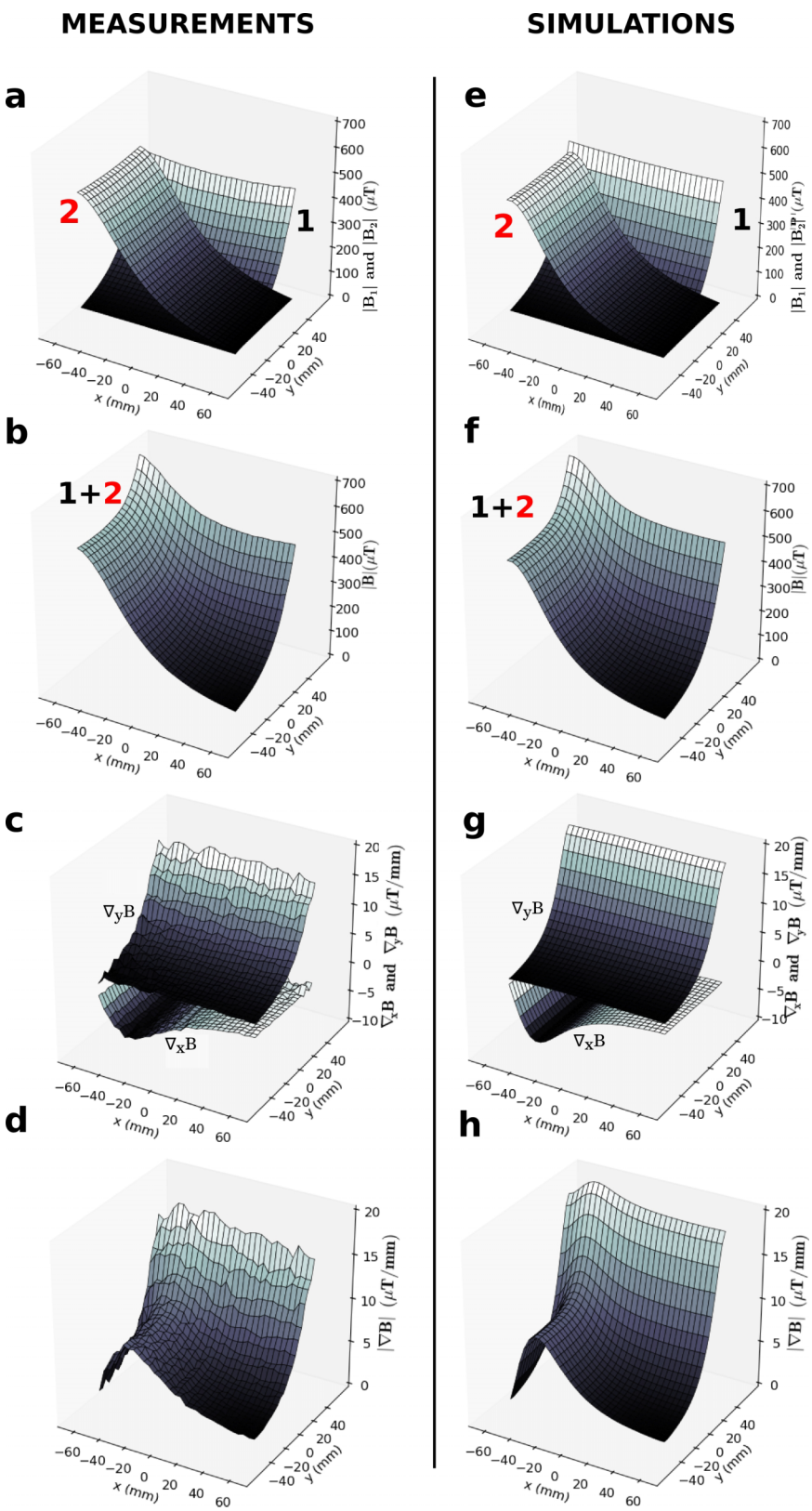

FIG. 5. (a): Measured field strength of the two coils ($|\mathbf{B}_1|$ and $|\mathbf{B}_2|$) injected with 1 A (average over five measurements) are plotted together. (b): Vector addition of the fields ($|\mathbf{B}|$) plotted in (a). (c): Field gradient main components ($\nabla_x B$ and $\nabla_y B$) and (d): Intensity of their vector addition $|\nabla \mathbf{B}|$. (e)-(h): Simulated versions of (a)-(d), respectively.

loads. In order to test this thermal stress, measurements of the temperature were done at wells A1 (worst case scenario), A7, and E1. The temperature elevation course was evaluated using an LM53 precision centigrade temperature sensor (Texas Instruments, Dallas, TX) located inside the tested well, which was filled with water to better mimic the situation of an experiment with cells. In this regard, the exact thermal response of diverse culture media could differ among each

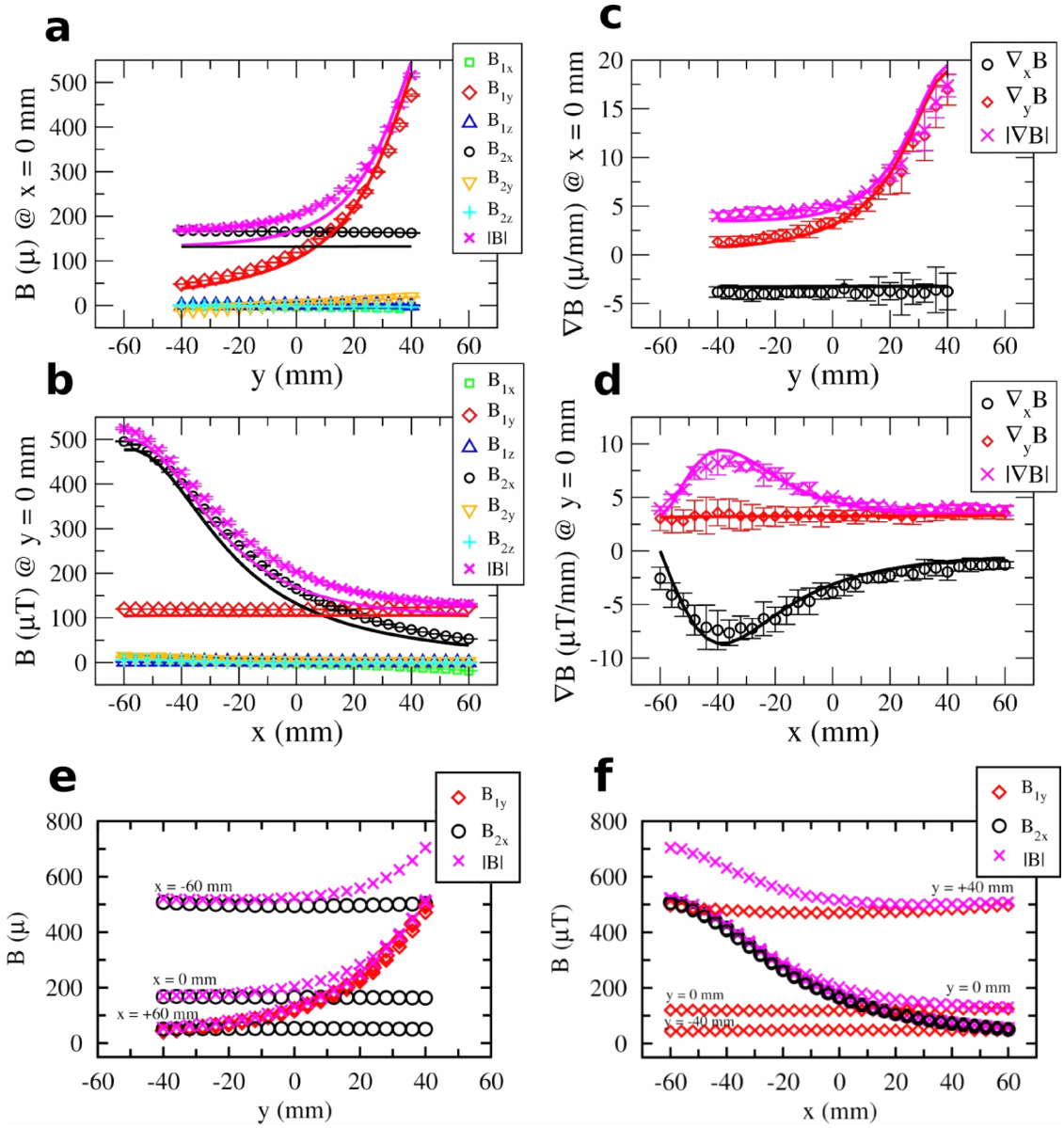

FIG. 6. (a) and (b): Continuous lines correspond to the calculated values, while symbols correspond to measured values (average over five measurements ±SD). The three components of the field generated by each coil and the field strength are plotted for the planes at x = 0 mm and y = 0 mm, respectively. (c) and (d): Same as (a) and (b) but for the main components of the gradient ($\nabla_x B$ and $\nabla_y B$) and its intensity ($|\nabla \mathbf{B}|$). Also, the main components (B_{1y}, red diamonds, and B_{2x}, black circles) and the total intensity (magenta crosses) for x = −60, 0, and +60 mm, and for y = −40, 0, and +40 mm are plotted in (e) and (f), respectively. As expected, the three curves for B_{1y} (in (e)) and for B_{2x} (in (f)) are practically coincident.

other and from that of water. Hence, experimenters should test temperature loads using the exact culture media that will be used in their experiments. The microplate (with its lid on) was positioned in the apparatus with the coils unenergized, inside an incubator set at 37 °C and with a high humidity, and the whole system was left to thermalize for several hours. Next, 1 A DC current was injected to both coils (connected in series). Measurements were taken automatically every 10 min with a 6½ digital multimeter Agilent 34410A (Agilent, Santa Clara, CA) connected to a PC, for up to 8 h. Figure 7 shows the time course of temperature (the current was turned on at time = 1 h).

Since measurements were done in subsequent days and the incubator was opened and closed after each curve acquisition (for repositioning the sensor), it is natural that the initial baseline-temperature was not identical for all the curves. Temperature elevations (Δ) were found to be: $\Delta_{A1(1\ A)} \sim 0.65$ °C, $\Delta_{A7(1\ A)} \sim 0.47$ °C, and $\Delta_{E1(1\ A)} \sim 0.42$ °C; and $\Delta_{A1(0.6\ A)} \sim 0.21$ °C. Now, considering that a typical temperature uniformity deviation (in space) inside a commercial cell culture CO_2 incubator is ±0.25 °C (Panasonic MCO-18AC, Wood Dale, IL), the recorded temperature elevations for 1 A are to be considered excessive. However, injecting 0.6 A to both coils yields an acceptable temperature load, and so the system should only be used with currents up to this value. In this regard, it is appropriate to remember here that increasing the number of windings (N) of the coils improves the field generation to Joule effect ratio. For example, if N is doubled (N → 2N), then the necessary current to produce a certain field will be divided by 2 (I → I/2), while the resistance

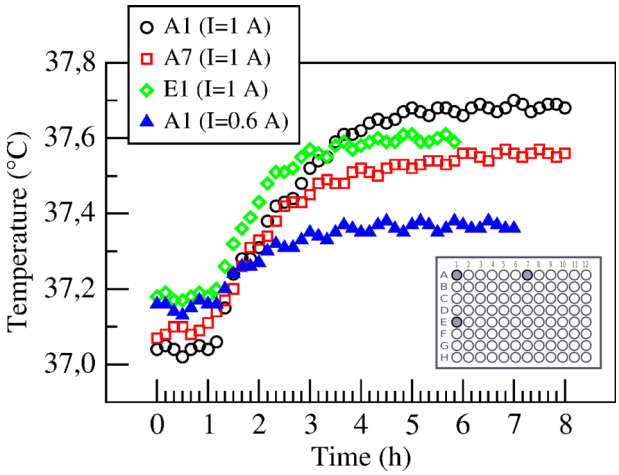

FIG. 7. Time course of the temperature at wells A1, A7, E1 for I = 1 A and A1 for I = 0.6 A. The lower-right corner shows a 96 wells microplate with wells A1, A7, and E1 highlighted.

will double (R → 2R). Hence, the heating power will divide by 2: $I^2R \rightarrow (I/2)^2(2R) = (I^2R)/2$.

Tables S1 to S4 (supplementary material) show representative values for a current of 1 A, so they can easily be scaled multiplying them by the current used in each experiment. For the maximum acceptable current of 0.6 A (injected to both coils), the generated fields would be in the range of ~350 μT (A1) to ~43 μT (H12). The maximum field gradient for 0.6 A happens at A3 and is of 9 μT/mm.

IV. DISCUSSION

Firstly, it should be clear what is the main contribution intended with the present work: to present an apparatus that could sensibly accelerate exploration of *in vitro* bioeffects in magnetobiology. This is so because different fields could be evaluated almost 100 times (96, to be exact) faster than evaluating one by one in standard, homogeneous field experiments. Besides this key feature, advantages and disadvantages are discussed next.

Upon a little analysis, it becomes clear that any system of coils that would produce an inhomogeneous field throughout the surface of a multi-well microplate would allow the simultaneous study of a range of field intensities. However, provided only one of the coils is energized, the proposed design presents the advantage of producing isolines of fields parallel to the rows (or the columns). In that way, statistics will be more robust since, for instance, if only coil 1 is energized, then each field value will be tested in 12 wells. While this is clearly not equivalent to performing 12 repeats of the experiment, it does reinforce statistics. In case of injecting currents to both coils, that statistical gain is lost in exchange of evaluating many more different field intensities per experiment.

The measured field gradients deserve some special attention, since they reach values as high as ~17.5 μT/mm (close to row A of the microplate, Fig. 6(c)). Now, considering that a well's diameter in a 96 microplate is 6.35 mm, the measured gradient of 17.5 μT/mm implies a difference greater than 110 μT (~17.5 μT/mm × 6.35 mm) between the fields affecting cells lying in the upper (proximal) and lower (distal) edges of the same well. Although this variability within each of the wells decreases towards well H12, it should be taken into account at the time of interpreting results. For instance, if positive findings were found along, say, row A, it would be desirable to repeat the experiment injecting a greater current, so that the range of fields present in the wells of row A in the first experiment would now be spread throughout more rows (say, C through E). Complementary, experiments using homogeneous fields (no gradient at all) would clear doubts about the causal origin (field intensity and/or gradient) of the observed effects.

In regards to the possible number of wells of the microplate, standard quantities are 6 (2 × 3), 24 (4 × 6), 96 (8 × 12, the one used in this work), 384 (16 × 24), and 1536 (32 × 48). The advantage of increasing the number of wells is to increase the spatial resolution of experiments and to reduce the variation of the field within each well. However, it is technically more cumbersome to deal with a greater number of wells, and biological variability can become a problem (out of growing a smaller number of cells per well). Also, it must be taken into account that using microplates with a low number of wells (say, 6 or 24) implies that there will be even more important variations of the field inside each well. This could imply different degrees of biological effects (or even different biological effects) inside the same well, information that would be lost if the utilized bioeffect essay does not allow for spatial resolution. An interesting possibility in this respect is the well area scanning feature of the Epoch microplate spectrometer (Biotek, Winooski, VT). For instance, this feature could be used for quantifying cell viability with spatial resolution within each well. It is worth noting that microplates with fewer wells (and consequently bigger ones) would allow experiments with small model animals such as C. elegans[25–27] and Planarians[18,28] where, we emphasize, the interpretation of any finding should take into careful consideration the non-negligible field variations within each well.

As an example of the use of the apparatus, the experiments by Binhi *et al.*[17] on E. coli, with SMF between 0 and 110 μT, could be further developed: By injecting 0.6 A to both coils, the same bioeffect could be tested with fields between ~350 μT (A1) and ~43 μT (H12) (Table S3, supplementary material), partially overlapping (range from 43 μT to 110 μT) but further exploring their results (range from 110 μT to 350 μT). We emphasize here that the exploration of the whole range would be done in a single experiment.

Of note, is that injecting a 0.2 A current to coil 2, fields between ~91 μT (column 1) and ~12.6 μT (column 12, Table S2, supplementary material) could be generated. These values are of particular interest, since they include the whole range for the geomagnetic field (23 μT–65 μT). Hence, geomagnetic conditions for the whole globe can be roughly reproduced in a single microplate, during a single experiment. However, it should be noticed that not only field intensities, but also field directions will vary throughout the microplate when both coils are energized.

In any case, when conducting experiments with the apparatus, the Earth's MF and the incubator's background[20] field must be taken into consideration. Further, it will be important

that a sufficient number of repeats be performed in order to have a proper statistical power that would account for variability within cell culture work. These repeats, coupled with as many as 96 separate wells, will create a considerable bulk of data, potentially posing a handling and analysis problem. Therefore, before the biological work is undertaken, the statistical tools to be used should be carefully examined and their statistical power estimated (more than the conventional minimum of 3 repeats could well be needed if the power is to become adequate).

Given that field gradients in the apparatus are not zero, if a bioeffect was observed, complementary experiments using homogeneous fields would be highly desirable in order to determine whether the effect is due to the field intensity, its gradient, or the combination of both.

Due to the fact that intensities in the range of mT are of interest in magnetobiology, and that the maximum intensity reachable by the presented device—without producing excessive temperature loads—is of 350 μT, discussion of a possible upgrade is in order. The starting point here is the highest acceptable power dissipation. Above, in Sec. III D, it was shown that 0.6 A is the highest acceptable current, which implies a power dissipation of 216 mW (total resistance R_t = 0,6 Ω). Simple calculations yield that with N = 300 turns and I = 0.22 A, R_t = 4.5 Ω, P = 218 mW, and the generated field is greater than the one generated here (350 μT) by a factor of 2.75: (300 turns/40 turns) × (0.22 A/0.6 A); yielding a field $B_{max} \sim 963$ μT. Alternatively, a thicker wire (hence, lower resistance per unit length) could be used in order to reduce the number of turns. For instance, N = 200 of AWG 12 wire (~2 mm diameter) along with I = 0.35 A yield P = 207 mW and $B_{max} \sim 1020$ μT. In any case, it should be noticed that accommodating hundreds of turns would demand changing the dimensions of the coils, which in turn would change the exact field distribution in space. Therefore, it is recommended to (a) run simulations of any new design before actually building it, and (b), once the system is built, to measure the actual temperature load in the most compromised wells of the microplate.

Another aspect to bear in mind in a possible upgrade of the device is that, given the fact that a magnetobiological effect could depend on the direction of the field, it is desirable to minimize B_z. While it was shown that $B_x \sim B_y \gg B_z$ holds for the presented device, such condition could be further improved by simply enlarging the coils' dimensions (the chamber of the CO_2 incubator—provided one is used—will of course set the size limit).

Finally, it must be mentioned that (just as with any coil or system of coils) not only DC currents, but also alternate currents (AC) could be injected into the apparatus, thus producing AC magnetic fields. It is clear that the use of pure AC or the combination of DC and AC currents would greatly expand the possible field combinations to produce with the device.

V. CONCLUSION

A system consisting of two coils was designed, simulated, built, and fully characterized with DC currents. To the best of the author's knowledge, the presented configuration of two flattened orthogonal coils for *in vitro* experiments in magnetobiology has not been published elsewhere before. The novel apparatus presents the main advantage of allowing the testing of multiple field exposures in a single experiment, sensibly increasing the efficiency of a research program that would be interested in exploring a range (instead of a single value) of the field's parameters. Moreover, a concrete experiment was proposed to further investigate results found in the literature. The system does present the disadvantage of producing field gradients, whose bio-effects (if any) turn out, *a priori*, indistinguishable from those of the field intensity. Therefore, the presented system produces a valuable tool for *in vitro* magnetobiology research that, nevertheless, would certainly benefit from combining with already well-known homogeneous-field generating devices in order to separate the "intensity" and "gradient" variables.

SUPPLEMENTARY MATERIAL

See supplementary material for tables of magnetic field and magnetic field gradients.

ACKNOWLEDGMENTS

The author appreciates valuable technical discussions regarding the apparatus with Mr. Carlos Sosa Flores, Electronic Engineer Carlos Devia, Dr. Octavio Furlong, and Dr. Marcelo Nazzarro. This work was funded by the Consejo Nacional de Investigaciones Científicas y Técnicas, Argentina (CONICET, Grant No. PIP 112-201101-00615) and the Universidad Nacional de San Luis, Argentina (Grant No. PROICO 3-10314).

[1]V. N. Binhi, *Magnetobiology, Underlying Physical Problems* (Elsevier Science, Ltd., Bath, UK, 2002), p. 314.
[2]A. F. McKinlay, "More research is needed to determine the safety of static magnetic fields," Prog. Biophys. Mol. Biol. **87**, 173–174 (2005).
[3]R. H. W. Funk, T. Monsees, and N. Özkucur, "Electromagnetic effects—From cell biology to medicine," Prog. Histochem. Cytochem. **43**, 177–264 (2009).
[4]W. W. Campos Albuquerque, R. M. Pedrosa Brandão Costa, T. Salazar e Fernandes, and A. L. Figueiredo Porto, "Evidences of the static magnetic field influence on cellular systems," Prog. Biophys. Mol. Biol. **121**, 16–28 (2016).
[5]M. Z. Akdag, S. Dasdagm, A. K. Uzunlar, E. Ulukaya, A. Y. Oral, N. Çelik, and F. Akşen, "Can safe and long-term exposure to extremely low frequency (50 Hz) magnetic fields affect apoptosis, reproduction, and oxidative stress?," Int. J. Radiat. Biol. **89**, 1053–1060 (2013).
[6]M. A. Trillo, M. A. Martínez, M. A. Cid, and A. Úbeda, "Retinoic acid inhibits the cytoproliferative response to weak 50 Hz magnetic fields in neuroblastoma cells," Oncol. Rep. **29**, 885–894 (2013).
[7]M. E. Mognaschi, P. Di Barba, G. Magenes, A. Lenzi, F. Naro, and L. Fassina, "Field models and numerical dosimetry inside an extremely-low-frequency electromagnetic bioreactor: The theoretical link between the electromagnetically induced mechanical forces and the biological mechanisms of the cell tensegrity," Springerplus **3**(1), 473 (2014).
[8]J. Wang, S. She, and S. Zhang, "An improved Helmholtz coil and analysis of its magnetic field homogeneity," Rev. Sci. Instrum. **73**, 2175–2179 (2002).
[9]J. Schuderer, W. Oesch, N. Felber, D. Spät, and N. Kuster, "*In vitro* exposure apparatus for ELF magnetic fields," Bioelectromagnetics **25**, 582–591 (2004).
[10]K. Wójcik, J. Kaszuba-Zwoińska, E. Rokita, P. Thor, P. Chorobik, Z. Nieckarz, and J. Michalski, "Influence of magnetic fields on U937 cells viability," IFMBE Proc. **37**, 1311–1314 (2011).
[11]E. Calabrò, S. Condello, M. Currò, N. Ferlazzo, D. Caccamo, S. Magazù, and R. Ientile, "Effects of low intensity static magnetic field on FTIR spectra

and ROS production in SH-SY5Y neuronal-like cells," Bioelectromagnetics **34**, 618–629 (2013).
[12]M. Ikehata, T. Koana, Y. Suzuki, H. Shimizu, and M. Nakagawa, "Mutagenicity and co-mutagenicity of static magnetic fields detected by bacterial mutation assay," Mutat. Res., Fundam. Mol. Mech. Mutagen. **427**, 147–156 (1999).
[13]M. Iwasaka, M. Ikehata, J. Miyakoshi, and S. Ueno, "Strong static magnetic field effects on yeast proliferation and distribution," Bioelectrochemistry **65**, 59–68 (2004).
[14]M. J. McLean, R. R. Holcomb, A. W. Wamil, J. D. Pickett, and A. V. Cavopol, "Blockade of sensory neuron action potentials by a static magnetic field in the 10 mT range," Bioelectromagnetics **16**, 20–32 (1995).
[15]S. Hughes, A. J. El Haj, J. Dobson, and B. Martinac, "The influence of static magnetic fields on mechanosensitive ion channel activity in artificial liposomes," Eur. Biophys. J. **34**, 461–468 (2005).
[16]C. Vergallo, M. Ahmadi, H. Mobasheri, and L. Dini, "Impact of inhomogeneous static magnetic field (31.7–232.0 mT) exposure on human neuroblastoma SH-SY5Y cells during cisplatin administration," PLoS One **9**(11), e113530 (2014).
[17]V. N. Binhi, Ye. D. Alipov, and I. Ya Belyaev, "Effect of static magnetic field on E. coli cells and individual rotations of ion-protein complexes," Bioelectromagnetics **22**, 79–86 (2001).
[18]V. V. Novikov, I. M. Sheiman, and E. E. Fesenko, "Effect of weak static and low-frequency alternating magnetic fields on the fission and regeneration of the planarian dugesia (girardia) tigrina," Bioelectromagnetics **29**, 387–393 (2008).
[19]V. N. Binhi, "A primary physical mechanism of the biological effects of weak magnetic fields," Biophysics **61**, 170–176 (2016).
[20]L. A. Portelli, T. E. Schomay, and F. S. Barnes, "Inhomogeneous background magnetic field in biological incubators is a potential confounder for experimental variability and reproducibility," Bioelectromagnetics **34**, 337–348 (2013).
[21]L. Kaufman, J. W. Carlson, B. McCarten, S. Krasnor, W. K. M. Lu, M. Arakawa, and K. A. Derby, "Spatially orthogonal rectangular coil pair suitable for vertical magnetic field MRI system," U.S. patent 5663645 (2 September 1997).
[22]See https://store.arduino.cc for Arduino Online Store, 2016.
[23]See www.ngdc.noaa.gov for National Centers for Environmental Information, National Oceanic and Atmospheric Administration, 2015.
[24]J. C. Lin, "Reassessing laboratory results of low-frequency electromagnetic field exposure of cells in culture," IEEE Antennas Propag. Mag. **56**, 227–229 (2014).
[25]T. Kimura, K. Takahashi, Y. Suzuki, Y. Konishi, Y. Ota, C. Mori, T. Ikenaga, T. Takanami, R. Saito, E. Ichiishi, S. Awaji, K. Watanabe, and A. Higashitani, "The effect of high strength static magnetic fields and ionizing radiation on gene expression and DNA damage in caenorhabditis elegans," Bioelectromagnetics **29**, 605–614 (2008).
[26]C.-H. Lee, Y.-C. Hung, and G. S. Huang, "Static magnetic field accelerates aging and development in nematode," Commun. Integr. Biol. **3**, 528–529 (2010).
[27]Z. Njus, D. Feldmann, R. Brien, T. Kong, U. Kalwa, and S. Pandey, "Characterizing the effect of static magnetic fields on C. elegans using microfluidics," Adv. Biosci. Biotechnol. **6**, 583–591 (2015).
[28]N. Gang and M. A. Persinger, "Planarian activity differences when maintained in water pre-treated with magnetic fields: A nonlinear effect," Electromagn. Biol. Med. **30**, 198–204 (2011).